



Multiscale modeling and prediction of elastic properties of MWCNT- and RHA-reinforced AIP0507 matrix composite

Nitin Srivastava¹ · Lavish Kumar Singh² · Manoj Kumar Yadav³ · Bodduru Kamesh¹

Received: 27 June 2023 / Accepted: 10 April 2024 / Published online: 3 May 2024

© The Author(s), under exclusive licence to The Brazilian Society of Mechanical Sciences and Engineering 2024

Abstract

The objective of this study is to utilize numerical modeling techniques to forecast the performance of a novel metal matrix composite and speed up the experimental testing process by reproducing the unique features observed at the micro-scale of the composite material. The matrix material chosen for this study was aluminum P0507 alloy, with multi-walled carbon nanotube (MWCNT) and rice husk ash (RHA) selected as the reinforcements. The reinforcement loading was varied from 1 to 9 vol.%. The representative volume element model in corroboration with the DIGIMAT-FE software was utilized to model, simulate and assess the performance of these composites across different volume fractions and orientations. Both the modulus, elastic and shear, increased monotonously with increase in the CNT and RHA content, whereas the Poisson's ratio decreased with increase in the reinforcement loading; the changes being more evident in CNT-reinforced composites. On one hand, highest value of E_1 was found in case of aligned inclusions, on the other hand, the highest value of E_2 and E_3 was found for composites containing 2D random orientation type inclusions. As far as shear moduli are concerned, the highest value of G_{12} was found for 2D random orientation type, and the highest value of G_{23} and G_{13} was found in case of 3D random type orientation. The elastic moduli and shear moduli followed the following trend: $E_1 > E_2 > E_3$ and $G_{12} > G_{13} > G_{23}$. The values of elastic as well as shear moduli for hybrid composite, Al-9 vol.% (CNT + RHA), were found to be higher than that of Al-9 vol.% RHA. For instance, the value of 2D-oriented E_1 increased from 77.15 to 78.40 GPa, and the value of aligned G_{13} enhanced from 29.17 to 29.45 GPa. Therefore, it can be concluded that hybrid composites give luxury to fabricate components with tailored properties at a lower cost.

Keywords Aluminum alloy P0507 · Multi-walled carbon nanotube · Rice husk ash · Representative volume element · Digimat · Elastic property

1 Introduction

In current automotive and aerospace industries, aluminum/MWCNT composites are valuable for their exceptional mechanical properties. Before 2004, MWCNT got little scientific and practical attention [1]. This 3D material has

sp²-hybridized carbon atoms with unique mechanical and physical properties. With a 100 GPa elastic modulus and 150 GPa tensile strength, MWCNT is outstanding. Due to its mechanical qualities, MWCNT is often used to reinforce composites. Metal/MWCNT and RHA hybrid composites have been studied. High heat conductivity makes MWCNT and RHA suitable composite fillers. Composite materials have a higher thermal conductivity due to RHA, MWCNT, and metal matrix bonding [2–4]. The low densities of MWCNT and RHA provide them with excellent specific strengths and moduli, making them suitable for reinforcing aluminum and subsequently prepare hybrid composites. With this knowledge, more research has been done on the fabrication and mechanical examination of composite materials such as (MWCNT/Al), (RHA/Al), and (MWCNT/RHA/Al) composites.

Technical Editor: Samikkannu Raja.

✉ Lavish Kumar Singh
lavish.singh2011@gmail.com

¹ Department of Mechanical Engineering, Sharda University, Greater Noida, Uttar Pradesh, India

² School of Engineering, Jawaharlal Nehru University, New Delhi 110067, India

³ Department of Mechanical Engineering, Ajay Kumar Garg Engineering College, Ghaziabad, Uttar Pradesh, India

Automotive, marine, aerospace, and electrical industries use aluminum and hybrid composites [5–7]. Strength, corrosion resistance, thermal efficiency, low thermal expansion coefficient, electrical resistivity, and damping capacity are exceptional in these composites [8–12]. Aluminum alloys are employed in airframes, wing airfoils, and other aviation parts, making them vital [13, 14]. More robust, more complex, and wear-resistant aluminum and hybrid composites have been made [15–17]. For aluminum and hybrid composites, solid- and liquid-state manufacturing processes are used. Recently, aluminum has been strengthened using carbon nanotubes (CNTs) [18]. Despite significant Al/CNT composite research, CNT uniform dispersion in the aluminum matrix remains difficult. Due to its two-dimensional nature, RHA distributes evenly in matrices. Producing Al/RHA composites has prospective application benefits. The alloying and stirring stir-casting procedure evenly distributes reinforcements in the aluminum matrix [19]. Sahu et al. [20] explained stir-casting in detail. Melting the matrix material, stirring the molten metal with a mechanical stirrer, incorporating the reinforcement material, continuous stirring, pouring the mixture into a mold, and solidifying the mixture produce composite and hybrid materials with excellent mechanical properties. Wear resistance, physical parameters, and microstructure of AlP0507 were assessed to evaluate the composites. Mechanical behavior simulation and modeling of these materials have also been studied. There are very few research publications on this topic, suggesting that it is still developing. To anticipate mechanical behavior, computational modeling of Al/MWCNT, Al/RHA, and Al/MWCNT/RHA hybrid composite materials is growing. Numerical modeling of CNT/Al composites to predict mechanical behavior is another growing subject [21, 22]. This study complements MWCNT/RHA/Al hybrid composite computational and experimental studies. Al/MWCNT composites and Al/MWCNT/RHA hybrid composites' mechanical characteristics are also studied utilizing experimental, analytical, and numerical simulation methods [23]. For instance, Zeng et al. [24] created a micromechanical finite element model to evaluate MWCNT's effect on the mechanical characteristics of Al/MWCNT composites.

There has been very limited numerical study discussing the elastic properties of MWCNT, Al, and RHA hybrid metal composites at different volume fractions. The fiber growth method may create RVEs with scattered and discontinuous fibers, according to Tian et al. [25]. Zhao et al. [26] analyzed carbon fiber-reinforced hydroxyapatite composites and found that the artificial bone mechanical characteristics improved as a result of carbon fiber addition. Complex 3D models were created using ABAQUS plug-in. This work generated periodic RVEs from composites with randomly dispersed short cylindrical fibers using numerical homogenization and modified RSA technique. The work showed strain and stress

fields on RVE barriers as seamless using ABAQUS with periodic boundary conditions. In another study, numerical homogenization's effective elastic characteristics and actual observations were found very close, proving its suitability for assessing composites reinforced with randomly dispersed short fibers [27]. In Enrique García-Macías' approach, elastic properties of CNT-reinforced polymer composites were determined. Atomic-based nanomodeling was used in the study [28]. The research showed that filler volume, chirality, and aspect ratio significantly altered the macroscopic reaction of the composites. Kavvadias et al. [29] also used the RVE model to carry out mechanical characterization under both tension and compression of MWCNT-reinforced cement paste.

This work investigates the elastic mechanical characteristics of aluminum metal matrix composites reinforced with MWCNT and RHA at varied volume fractions, separately and in hybrid combinations. At different volume fractions, RVEs were used to model and simulate Al/RHA, Al/MWCNT, and Al/RHA/MWCNT composites. For MWCNT/RHA-reinforced aluminum composites, FEA and DIGIMAT-FE software were used to simulate and model their behavior. DIGIMAT-FE constructed a 3D elemental RVE model of randomly oriented MWCNT/RHA-reinforced metal matrix composites. To aid future study and the design of comparable metal matrix composites, the simulation predicted the elastic characteristics of the considered composites.

2 Materials and methods

2.1 Materials

Rice husk ash: Rice husks, commonly regarded as agricultural waste and an environmental hazard, can be converted into rice husk ash fillers. When rice husks are burned outside the rice mill, two forms of ash are produced, which can be utilized as plastic fillers. Using RHA as a soil stabilizer presents an environmentally beneficial alternative to ultimate disposal. RHA is a cost-effective substitute for ceramic reinforcing materials like Al_2O_3 , AlN, TiC, SiC, etc. Recent studies have revealed that RHA contains 85% to 90% amorphous silica, which can replace silica in various ceramic applications. Heating silica results in the development of a crystalline form. To prepare the rice husk, it is washed with water to remove any unwanted dust and then allowed to dry at room temperature for a day. Subsequently, the rice husk is heat-treated at 200 °C for 60 min to eliminate moisture and organic matter. The color of the rice husk changes from yellowish to black as the organic content is burned off during heating. The resulting burnt ash contains significant silica, making it a strengthening material for composite fabrication. It has been determined that various factors, such as the

incineration method, heating rate, type of crop, and fertilizer used in rice farming, influence the characteristics of the ash and the burning conditions.

Multi-walled carbon nanotube: MWCNTs are formed by the arrangement of several single-walled carbon nanotubes within one another. They have concentric graphene layers with diameters ranging from 10 to 20 nm and lengths ranging from hundreds of microns to several millimetres. The layers in MWCNTs are spaced approximately 0.34 nm apart. Compared to mild steel with a tensile strength of 0.5 GPa, MWCNTs exhibit a much higher tensile strength of 10 to 50 GPa, making them significantly stronger when subjected to tension. The exceptional mechanical properties of MWCNTs make them suitable for use as reinforcing materials. However, achieving a homogeneous dispersion of MWCNTs in a metal matrix composite is a primary challenge. The effective dispersion and distribution of MWCNTs throughout the matrix material are crucial for achieving high-performance composites. Carbon nanotubes, including MWCNTs, have many current and potential applications. They can be incorporated into various materials to enhance existing properties or provide new capabilities. In particular, multi-walled carbon nanotubes can be used to increase the strength of components or achieve the same strength with less material, resulting in reduced weight.

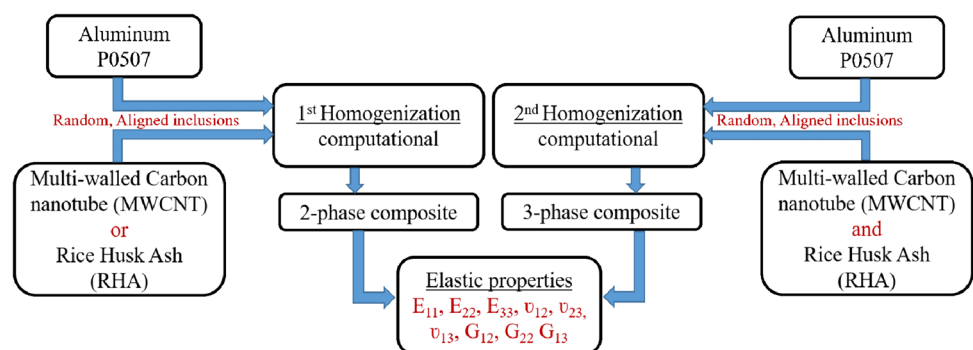
Aluminum P0507: Aluminum, specifically the P0507 alloy, is a lightweight metal with a silvery-white appearance. It is known for its flexibility and softness, allowing it to be easily bent and shaped. Aluminum finds application in various products, including cans, foil, kitchen utensils, window frames, beer kegs, and components in the aerospace industry. Its versatility stems from its unique properties. In the aerospace industry, aluminum is extensively used for various purposes, such as airplane frames, exteriors, wiring, and electrical systems. Its ability to form alloys by combining with other metals and its resistance to corrosion makes it highly suitable for these applications. The transportation and automotive industries also benefit from aluminum's desirable properties. One of the critical characteristics of aluminum is its non-corrosive nature, which contributes to its long-lasting durability. It can be

easily cast and machined into different shapes and sizes, offering versatility in manufacturing processes. Aluminum is lightweight, making it an ideal choice for applications where weight reduction is essential. Additionally, it is non-sparking and non-magnetic, further expanding its usability. Moreover, aluminum exhibits excellent thermal and electrical conductivity, allowing for efficient heat dissipation and effective electrical conduction.

2.2 Multiscale modeling and simulation

Multiscale computer modeling plays a crucial role in understanding how microstructural variables impact the mechanical properties of materials and guide the production of composite materials. Finite element analysis (FEA) is a computational method which has been used with the Digimat software. The Digimat-MF module is specifically designed for limited element-based homogenization, which estimates the elastic properties of composites based on their constitutive equations. Digimat-FE utilizes a RVE approach, placing integration points at the midpoint of the RVE. This study predicted the elastic properties of metal matrix composites using micromechanical properties and numerical simulations of composites reinforced with aligned and randomly distributed RHA and MWCNT. Figure 1 depicts a multiscale analysis of the homogenization process for two- and three-phase metal matrix composites. The focus was on evaluating the orthotropic elastic properties. These properties include the uniaxial Young's modulus (E_{11}), the in-plane Young's moduli (E_{22} and E_{33}), transverse Poisson's ratio (ν_{12}), and the in-plane Poisson's ratios (ν_{23} and ν_{13}), as well as the transverse shear modulus (G_{12}) and the in-plane shear moduli (G_{23} and G_{13}). To determine these properties, the isotropic properties (Young's modulus E , Poisson's ratio ν , and shear modulus G) of the metal matrix composites were converted into their respective directional properties ($E_1, E_2, E_3, \nu_{12}, \nu_{21}, \nu_{31}, G_{12}, G_{23},$ and G_{13}). This analysis provides valuable insights into the elastic behavior of metal matrix composites at different scales and helps in design and optimization of these materials.

Fig. 1 Multiscale analysis of two- and three-phase metal matrix composite homogenization



2.3 Computational model and RVE modeling

The elastic mechanical properties of metal matrix aluminum composites reinforced with RHA and MWCNT were investigated using RVEs created with Digimat-FE software. Three-dimensional computational microstructural models were utilized to assess various variables' effects on the composites' elastic properties, such as volume percentage, aspect ratio, randomly aligned inclusions, and the diameter-to-thickness ratio of MWCNT and RHA. In the simulation conducted, the components were precisely represented as three-dimensional solid parts to effectively capture and analyze their structural characteristics. To incorporate periodic boundary conditions, a rigorous meshing approach was implemented. The mesh was intentionally constructed to exhibit periodicity, ensuring the preservation of continuity and uniformity across the boundaries of the components. The usage of a periodic meshing approach facilitated the successful implementation of periodic boundary conditions, hence ensuring the faithful representation of the actual behavior of the components being investigated in the simulation. In the RVE models with randomly oriented and aligned inclusions, the MWCNT and RHA volume percentage was estimated in range from 1 to 9%. The MWCNT inclusions were modeled as cylinders with a thickness of 30 nm and an interface thickness of 5 nm. The interfaces between the metal matrix and nano-fillers play a crucial role in determining the mechanical characteristics of the composites. The width and alignment of the inclusions were kept constant in all three directions. Representative volume element depicting 2D random, 3D random, and 2D aligned inclusions in the aluminum matrix is shown in Fig. 2. The inclusions were assumed to be fully connected to the interface layers, ideally linked to the matrix. The elastic properties of the RVEs were determined using this modeling approach. Periodic boundary conditions (PBCs) in three dimensions represent an infinite material domain. Tetrahedral elements were used to mesh the RVE models, and the meshes contained millions

of elements depending on the number of inclusions. The finite element approach was implemented using the Digimat software. Table 1 provides the mechanical properties of the aluminum P0507 matrix, MWCNT, and RHA, which were used as input parameters to evaluate the orthotropic properties. For the 3D RVE models, a minimum mesh size of 5 nm was set, resulting in 1–2 million tetrahedral elements (C3D4). The periodic unit cell (PUC) model assessed the elastic properties. This model assumed a multi-layer structure with a single MWCNT flake of 30 nm thickness. These computational simulations and modeling techniques provide insights into the elastic behavior of the metal matrix composites and help understand the influence of different parameters on their mechanical properties.

$$\varepsilon_{ij} = \frac{1}{|\varphi_e|} \int_{\varphi} \varepsilon_{ij}^0(x, y) d\varphi_e \quad (1)$$

$$\sigma_{ij} = \frac{1}{|\varphi_e|} \int_{\varphi} \sigma_{ij}^0(x, y) d\varphi_e \quad (2)$$

$$\sigma_{ij} = C_{ijkl}^H(\varepsilon^0)(\varepsilon_{kl}) \quad (3)$$

where ε_{ij} and σ_{ij} are the volumes averaged strain and stress, respectively;

ε_{ij}^0 and σ_{ij}^0 are the local strain and stress, respectively;

φ_e is the total volume of the RVE;

Table 1 Mechanical properties of the materials used in the study

Materials	Young's modulus (GPa)	Poisson's ratio	Density (g/cm ³)
MWCNT	270	0.16	2.1
RHA	215	0.15	1.8
P0507	70	0.33	2.7

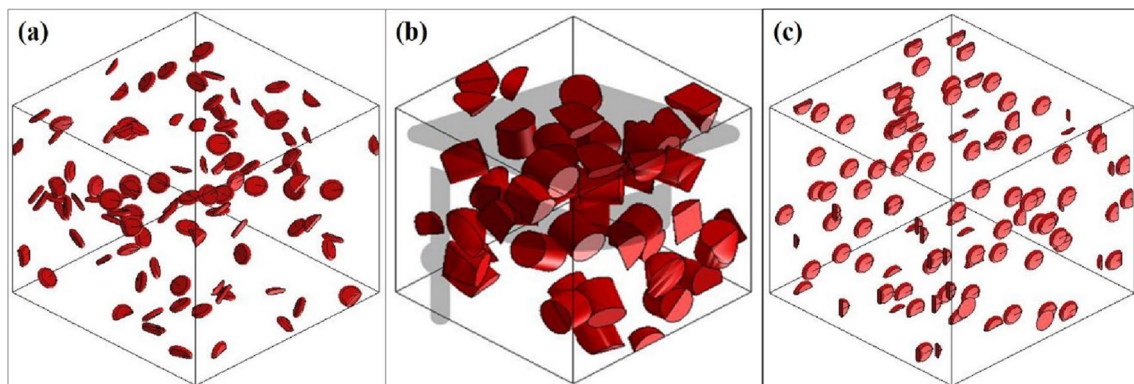


Fig. 2 Representative volume element depicting **a** 2D random, **b** 3D random, and **c** 2D aligned inclusions in aluminum matrix

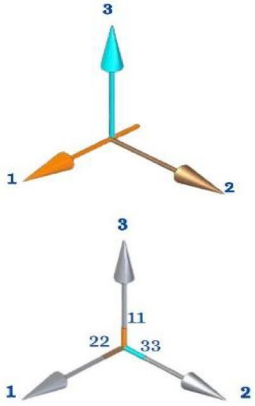
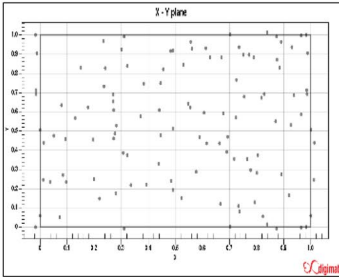
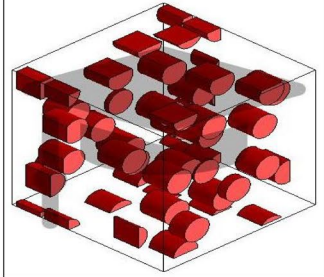
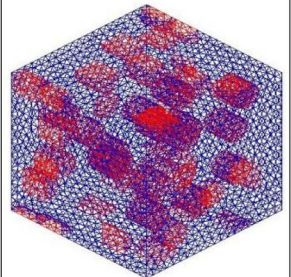
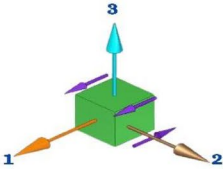
1. General parameters		
Analysis type: Mechanical Digimat FE-Homogenization		
2. Materials		
Nano filler Inclusion and metal matrix model	<ul style="list-style-type: none"> • Constitutive law: Elastic • Elasticity: Isotropic symmetry • Parameters: Density • Elastic parameters: Young’s modulus, Poisson’s ratio, and Shear modulus 	
3. Microstructure		
<ul style="list-style-type: none"> • The metal (phase type) is assigned as the matrix phase. • The MWCNT phase and RHA phase (phase type) – inclusion • Interface behaviour: perfectly bounded. • Phase fraction: volume fraction • Inclusion shape: (a) MWCNT-cylinder and (b) RHA-cylinder • Fixed aspect ratio • Orientation: $[\theta = 90^\circ \text{ and } \varphi = 0^\circ]$, 2D random, aligned, 3D random 		
4. RVE generation		
Periodic geometry	RVE geometry generation	RVE mesh geometry
		
Geometry inclusions distribution x,y plane	Inclusion + aluminum geometry	After mesh inclusion + aluminium geometry
5. Loadings		
<ul style="list-style-type: none"> ✓ Boundary condition: periodic ✓ Mechanical loading: (h) Uniaxial strain loading in direction 1 		
6. Results		
Graphs between E , ν and G with respect to volume fractions	<p>Engineering constants</p> <p>Random: E, ν, G, K, ρ</p> <p>Aligned: $E_1, E_2, E_3, \nu_{12}, \nu_{21}, \nu_{31}, G_{12}, G_{23}, G_{13}$</p>	

Fig. 3 An overview of the homogenization process

Table 2 Chemical composition of aluminum P0507

Element	Si	Fe	Mn	Mg	Cu	Zn	Ti	V	Ga	Na	Cr	Zr	Ni	Pb	Sr	Ca	Al
Weight %	0.0408	0.0584	0.0014	0.0005	0.0005	0.0020	0.0031	0.0129	0.0109	0.0020	0.0015	0.0004	0.0032	0.0010	0.0001	0.0001	99.88

Table 3 Properties of MWCNT and RHA reinforcements used in this study

Features	MWCNT	RHA
Thickness	25 nm	3.65 μm
Surface area	100 $\text{m}^2 \text{g}^{-1}$	1.246 $\text{m}^2 \text{g}^{-1}$
Diameter	0.05 μm	13.5 μm
Aspect ratio	1	2.495
Bulk density	80 kg/m^3	90 kg/m^3
Young's modulus	270 GPa	215 GPa
Strength	63 GPa	0.0384 GPa

C_{ijkl}^H is the equivalent homogenized stiffness matrix.

C_{ijkl}^H constants can be calculated by applying six microstrains and PBC for six independent models.

2.4 Micromechanical properties

The study conducted homogenization of aluminum matrix composites reinforced with MWCNT/RHA (two-phase composite) and MWCNT and RHA (three-phase composite) using the DIGMAT-FE software. The aim was to determine the elastic properties of the metal matrix composites. The DIGMAT-FE program created an RVE model of the MWCNT/RHA-reinforced metal matrix composites in a typical 3D elemental form. The MWCNT and RHA were cylindrical shapes with aligned and random orientations. Various physical characteristics of the MWCNT and RHA, such as volume fraction, aspect ratio, orientation, interfacial contact, and accumulation, can influence the elastic properties of the nanocomposite. In this study, the effect of only one parameter, volume fraction ratio of the nano-fillers, was investigated. The different phases involved in the composites, including aluminum with RHA and MWCNT nano-fillers, were considered as the general parameters for the homogenization process. An overview of the homogenization process is depicted in Fig. 3. By following these steps and utilizing the Digimat-FE software, the study aimed to obtain accurate predictions of the elastic properties of the considered metal matrix composites.

2.5 Material synthesis

In the experimental phase of the study, (Al + MWCNT), (Al + RHA) composites, and (Al + MWCNT + RHA) composites were produced using vacuum stir-casting process. The materials used included aluminum P0507 in solid form and MWCNT and RHA in powder form. Vacuum stir-casting method was chosen because it ensures the uniform distribution of the reinforcement within the matrix and helps

Fig. 4 Variation in elastic modulus of two-phase composites with varying **a** MWCNT and **b** RHA content

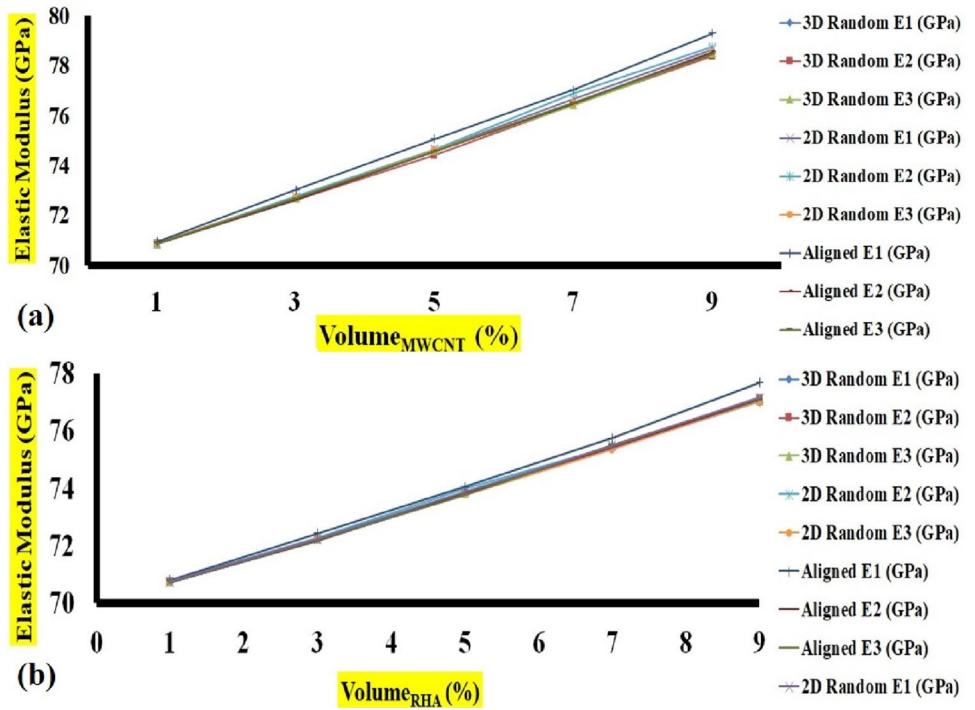
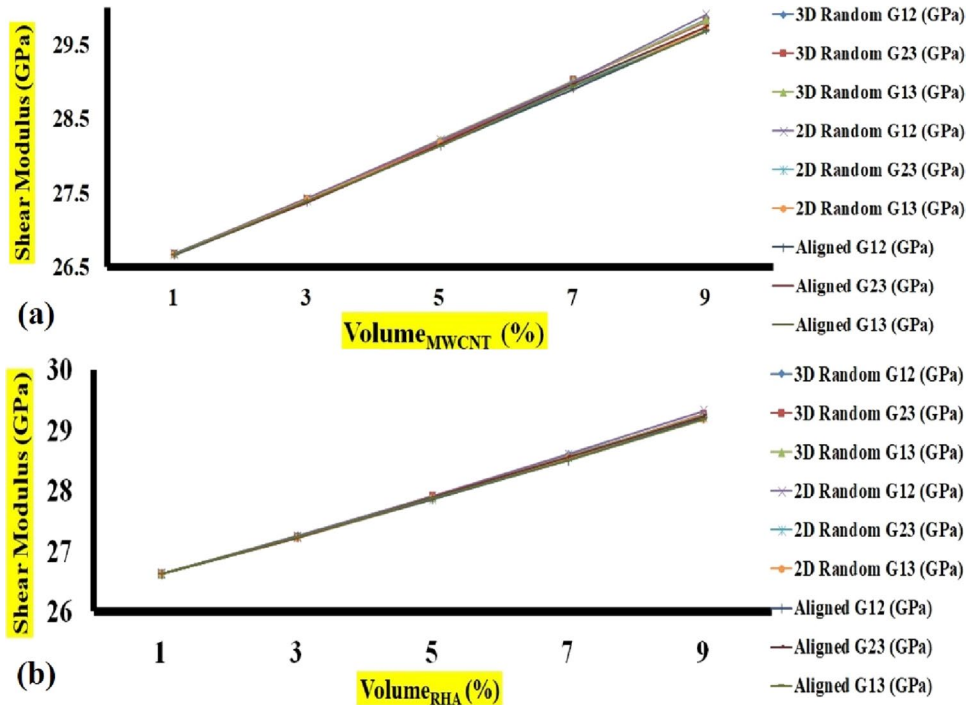


Fig. 5 Variation in shear modulus of two-phase composites with varying **a** MWCNT and **b** RHA content



minimize the formation of porosity in the casting material. It facilitates the segregation of the dispersed reinforcement throughout the molten matrix during the casting and melting

processes. Chemical composition of the aluminum alloy P0507 is shown in Table 2. Information regarding the characteristics of the MWCNT and RHA is illustrated in Table 3.

Fig. 6 Variation in Poisson’s ratio of two-phase composites with varying **a** MWCNT and **b** RHA content

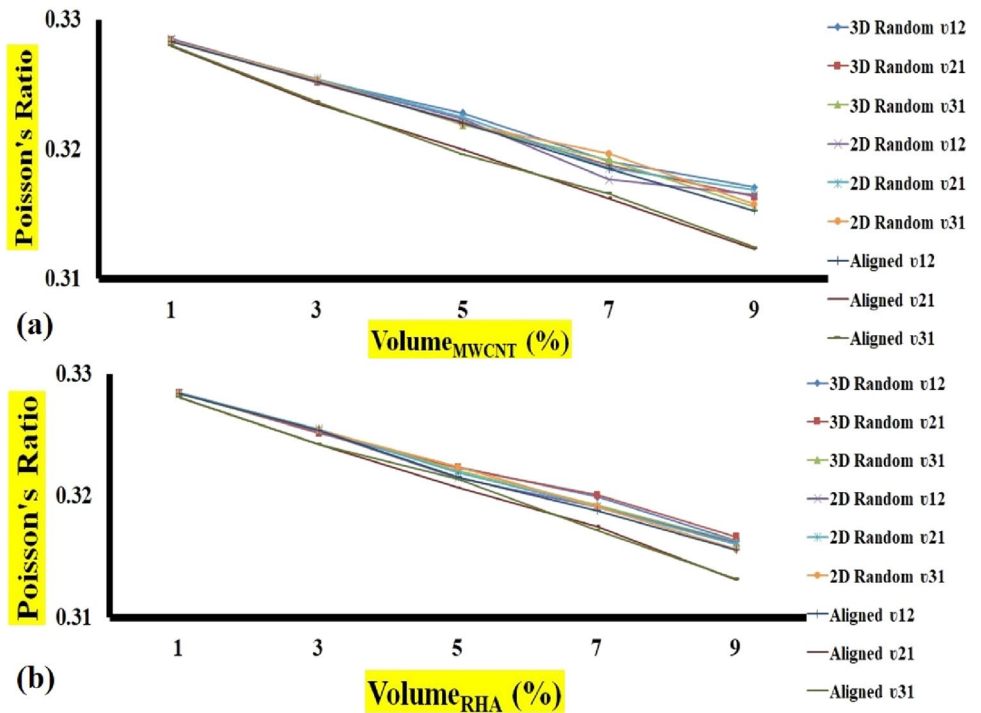


Table 4 Mechanical properties of Al/CNT and Al/RHA composites considering 2D random inclusion of the reinforcements

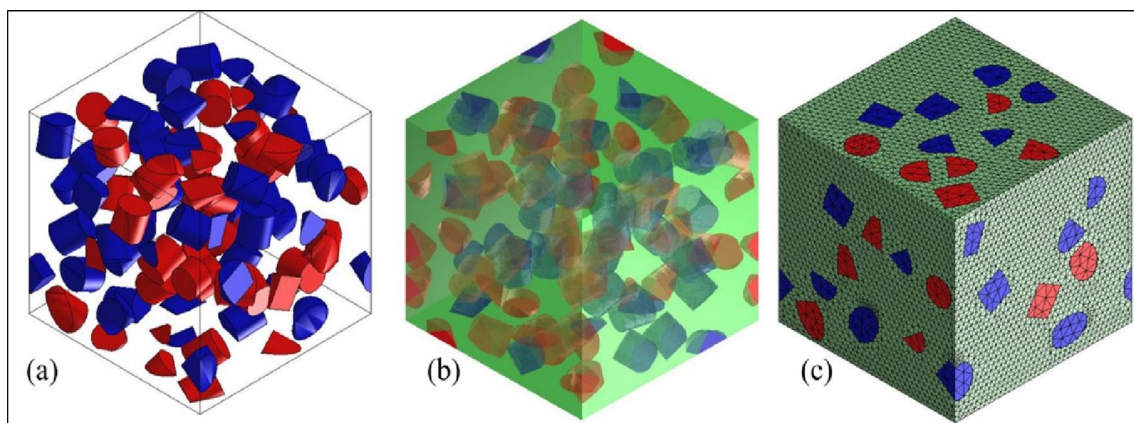
Composite	E_1 (GPa)	E_2 (GPa)	E_3 (GPa)	ν_{12}	ν_{21}	ν_{31}	G_{12} (GPa)	G_{23} (GPa)	G_{13} (GPa)
1 MWCNT + Al	70.9033	70.8767	70.8867	0.328503	0.328393	0.32833	26.685	26.667	26.6710
3 MWCNT + Al	72.7433	72.7667	72.7167	0.325320	0.325430	0.325327	27.4307	27.3920	27.4057
5 MWCNT + Al	74.6233	74.6600	74.6167	0.322273	0.322427	0.321937	28.2150	28.1667	28.1633
7 MWCNT + Al	76.6900	76.9100	76.5000	0.317620	0.318530	0.319643	29.0020	28.9500	28.9070
9 MWCNT + Al	78.6733	78.7667	78.5400	0.316440	0.316810	0.315710	29.9103	29.7380	29.7283
1 RHA + Al	70.7367	70.7333	70.7200	0.328437	0.328413	0.328373	26.6250	26.6133	26.6133
3 RHA + Al	72.2300	72.2600	72.2400	0.325323	0.325460	0.325400	27.2390	27.2197	27.2117
5 RHA + Al	73.8667	73.9633	73.7633	0.321467	0.321887	0.322343	27.8997	27.8540	27.8567
7 RHA + Al	75.4567	75.4567	75.3433	0.319063	0.319043	0.319060	28.5983	28.5380	28.5193
9 RHA + Al	77.1500	77.1100	77.0367	0.316157	0.315993	0.315577	29.3183	29.2020	29.1753

Table 5 Mechanical properties of Al/CNT and Al/RHA composites considering 3D random inclusion of the reinforcements

Composite	E_1 (GPa)	E_2 (GPa)	E_3 (GPa)	ν_{12}	ν_{21}	ν_{31}	G_{12} (GPa)	G_{23} (GPa)	G_{13} (GPa)
1 MWCNT + Al	70.8767	70.8833	70.8533	0.328377	0.328400	0.328363	26.6810	26.6723	26.6757
3 MWCNT + Al	72.6700	72.6333	72.6867	0.325303	0.325133	0.325377	27.4027	27.4170	27.4260
5 MWCNT + Al	74.5867	74.4233	74.6133	0.322757	0.322047	0.321840	28.1943	28.1860	28.2213
7 MWCNT + Al	76.5433	76.4600	76.4233	0.319087	0.318727	0.319160	29.0027	29.0193	29.0217
9 MWCNT + Al	78.5700	78.3900	78.5100	0.317030	0.316300	0.315480	29.8483	29.8113	29.8330
1 RHA + Al	70.7233	70.7200	70.7233	0.328430	0.328417	0.328477	26.6157	26.6177	26.6193
3 RHA + Al	72.2167	72.1800	72.2033	0.325297	0.325130	0.325440	27.2390	27.2270	27.2320
5 RHA + Al	73.8000	73.7900	73.7933	0.322343	0.322297	0.322077	27.8863	27.9003	27.8860
7 RHA + Al	75.3667	75.4000	75.4933	0.319887	0.320030	0.319223	28.5867	28.5490	28.5733
9 RHA + Al	77.0100	77.0867	77.0300	0.316280	0.316600	0.316177	29.2167	29.2580	29.2503

Table 6 Mechanical properties of Al/CNT and Al/RHA composites considering aligned inclusion of the reinforcements

Composite	E_1 (GPa)	E_2 (GPa)	E_3 (GPa)	ν_{12}	ν_{21}	ν_{31}	G_{12} (GPa)	G_{23} (GPa)	G_{13} (GPa)
1 MWCNT + Al	70.9567	70.8700	70.8800	0.328293	0.327897	0.327963	26.6630	26.6673	26.6710
3 MWCNT + Al	73.0267	72.6433	72.6900	0.325220	0.323517	0.323637	27.3803	27.3750	27.3967
5 MWCNT + Al	75.0733	74.5900	74.5700	0.321983	0.319917	0.319553	28.1370	28.1573	28.1350
7 MWCNT + Al	77.0533	76.4933	76.5267	0.318477	0.316183	0.316573	28.9077	28.9757	28.9437
9 MWCNT + Al	79.3133	78.5700	78.4667	0.315230	0.312293	0.312403	29.6973	29.7457	29.6760
1 RHA + Al	70.7900	70.7233	70.7200	0.328400	0.328093	0.328093	26.6133	26.6130	26.6140
3 RHA + Al	72.4300	72.1667	72.1833	0.325370	0.324197	0.324220	23.2307	27.2187	27.2253
5 RHA + Al	74.0333	73.8233	73.7600	0.321537	0.320643	0.321333	27.8567	27.8903	27.8690
7 RHA + Al	75.7367	75.4233	75.4867	0.318770	0.317463	0.317143	28.4987	28.5560	28.4930
9 RHA + Al	77.6667	77.0667	77.1167	0.315530	0.313097	0.313160	29.1953	29.2313	29.1733

**Fig. 7** Hybrid Al-9 vol.% (CNT/RHA) composite showing **a** random inclusions, **b** geometry, and **c** meshing

3 Results and discussion

In this part of the study, a computational model was developed to determine the elastic properties of an aluminum metal matrix composite reinforced with MWCNT and RHA in both aligned and random configurations. The focus was on investigating the effect of volume fraction on the elastic properties of the composite, considering an aspect ratio of 1 for both MWCNT and RHA. The literature values for Young's modulus (E) and Poisson's ratio (ν) of MWCNT, RHA, and aluminum were taken as 270 GPa, 0.16 for MWCNT; 215 GPa, 0.15 for RHA and 70 GPa, 0.33 for aluminum, respectively. These elastic properties served as input parameters to develop the orthotropic properties of the metal matrix composites consisting of MWCNT, RHA, and aluminum. Two scenarios were considered in the computational model. In the first scenario, aligned inclusions of MWCNT and RHA were incorporated into the aluminum matrix, and in the second scenario, random inclusions of MWCNT and RHA were incorporated into the aluminum

matrix. Digimat-FE software analyzed the three-directional properties, including the longitudinal properties, in-plane properties of Young's modulus, Poisson's ratio, and shear modulus, for the MWCNT- and RHA-reinforced aluminum metal composites. This computational model allowed for the assessment of the mechanical properties of two-phase and three-phase metal matrix composites, providing insights into the behavior of the composites under different configurations and volume fractions of the reinforcing materials.

3.1 First homogenization for two-phase composites

The computational modeling and analysis of the MWCNT and RHA-reinforced aluminum metal composites revealed several significant findings. Figures 4, 5, and 6 present the elastic modulus, shear modulus, and Poisson's ratio of the two-phase composites with varying MWCNT and RHA content. It can be observed that the elastic modulus increases monotonously with increase in the MWCNT and RHA

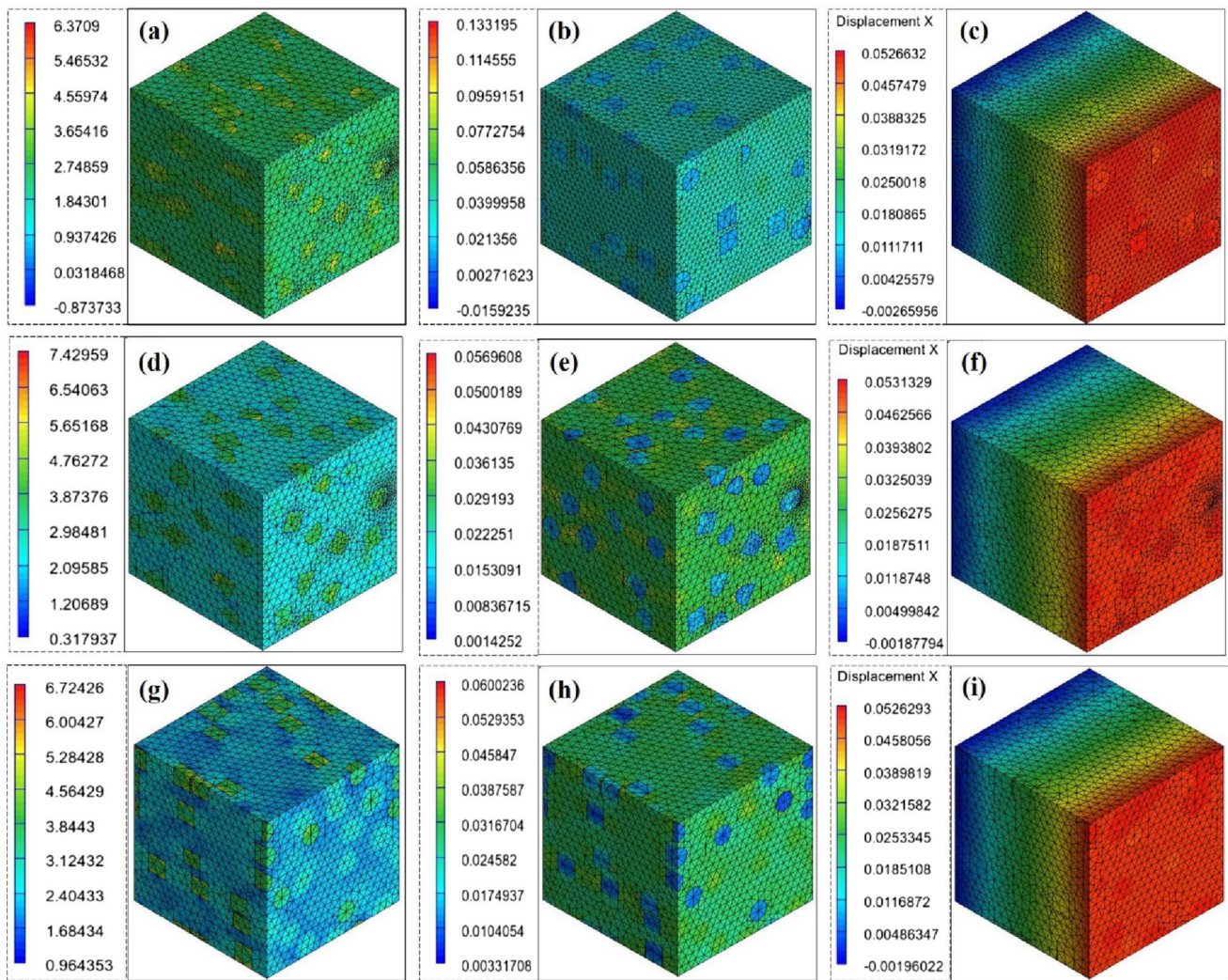


Fig. 8 Equivalent Von-Mises stress in (MPa), elastic strain and displacement (mm) of Al/CNT/RHA hybrid composite with inclusions orientated in **a–c** 2D random, **d–f** 3D random, and **g–i** aligned direction

Table 7 Elastic properties of Al/CNT/RHA hybrid composite with reinforcements dispersed in different orientations

Al-9 vol.% (CNT+RHA)	E_1 (GPa)	E_2 (GPa)	E_3 (GPa)	G_{12} (GPa)	G_{23} (GPa)	G_{13} (GPa)	ν_{12}	ν_{21}	ν_{31}
2D Random	77.86	77.83	77.85	29.53	29.43	29.37	0.319	0.319	0.317
3D Random	77.70	77.74	77.75	29.45	29.47	29.48	0.318	0.319	0.319
Aligned	78.40	77.77	77.84	29.39	29.45	29.45	0.317	0.315	0.321

loading from 0 to 9 vol.%. The maximum elastic modulus for both the types of composites was achieved for 9 vol.% reinforcement; value being ~79.3 GPa for Al/CNT composite and ~77.7 GPa for Al/RHA composite.

Mechanical properties of MWCNT/RHA-reinforced Al composite with 2D random inclusions, 3D random inclusions, and aligned inclusions are shown in Tables 4, 5, and 6, respectively. It can be clearly seen that both the modulus,

elastic, and shear increased monotonously with increase in the CNT and RHA content, whereas the Poisson's ratio decreased with increase in the reinforcement loading. However, it is noteworthy that the enhancement in modulus was more substantial in case of CNT reinforced composite.

Microstructural complexity and organization greatly impact mechanical properties. As far as E_1 is concerned, highest value was reported by aligned inclusions followed by 2D random and 3D random inclusions. Frącz and Janowski [30] while investigating the effect of fiber orientation on the strength properties of products made from wood-polymer composites also reported higher value of E_1 for random 2D type (1890 MPa) in comparison with the random 3D type (1825.68 MPa). However, the highest value of E_2 and E_3 was found for 2D random orientation type followed by aligned and 3D random. Elmarakbi et al. [31] while studying the properties of hybrid glass fibers/graphene platelets/PA6 composites also inferred that the aligned 2D distribution showed more effective reinforcement behavior as compared to the random 3D distribution. Also, in most of the case, the values of various elastic moduli followed the following trend irrespective of the reinforcement: $E_1 > E_2 > E_3$.

As far as shear moduli are concerned, on one hand, the highest value of G_{12} was found for 2D random orientation followed by 3D random and aligned orientations; on the other hand, the highest value of G_{23} and G_{13} was found in case of 3D random type orientation. It is notable that Al/CNT and Al/RHA composites containing aligned inclusions exhibited lowest shear moduli. Additionally, in most of the case, the values of various shear moduli followed the following trend irrespective of the reinforcement: $G_{12} > G_{13} > G_{23}$. The aligned configuration exhibited the lowest Poisson's ratios, be it ν_{12} , ν_{21} or ν_{31} for all the considered Al/CNT composites.

3.2 Second homogenization for three-phase composites

The elastic properties of a novel hybrid composite material comprised of CNT, RHA, and Al as a three-phase composite has been discussed in this section. In case of two-phase composites, 9 vol.% RHA and CNT gave the best elastic properties, therefore, for hybrid composite 4.5 vol.% each of CNT and RHA have been considered. By utilizing computational modeling using RVE approach, the study systematically evaluates the impact of orientations of MWCNT and RHA inclusions on the elastic properties of the hybrid composite. Schematic diagram depicting random inclusions, geometry, and meshing carried out in the hybrid composite is shown in Fig. 7.

Equivalent Von-Mises stress, elastic strain, and displacement experienced by the hybrid composite are illustrated in Fig. 8 for all the three orientation conditions, and

corresponding derived elastic properties is tabulated in Table 7. As far as elastic modulus is concerned, the highest E_1 was found in case of aligned inclusion orientation and the highest E_2 and E_3 were found in case of 2D random inclusion orientation. And for shear modulus, the highest G_{12} was found in case of 2D random orientation and the highest G_{23} and G_{13} were found in case of 3D random inclusion orientation. These findings are in line with the observations inferred for two-phase composites. The values of elastic as well as shear moduli for three-phase hybrid composite were found to be higher than that of Al-9 vol.% RHA. For instance, the value of 2D-oriented E_1 increased from 77.15 to 78.40 GPa, and the value of aligned G_{13} enhanced from 29.17 to 29.45 GPa. Therefore, it can be concluded that hybrid composites give luxury to fabricate components with tailored properties at a lower cost.

4 Conclusions

The study utilized numerical simulation through DIGIMAT software to predict the elastic properties of two-phase Al/CNT and Al/RHA composites and three-phase Al/CNT/RHA hybrid composite. The effect of reinforcement content and inclusion orientations (2D random, 3D random, and 2D aligned) on the elastic properties of the composites was investigated.

- It was observed that both the modulus, elastic and shear, increased monotonously with increase in the CNT and RHA content, whereas the Poisson's ratio decreased with increase in the reinforcement loading; the changes being more evident in CNT-reinforced composites.
- The highest value of E_1 was found for aligned inclusions, whereas the highest value of E_2 and E_3 was found for 2D random orientation type. The elastic moduli followed the following trend: $E_1 > E_2 > E_3$.
- As far as shear moduli are concerned, the highest value of G_{12} was found for 2D random orientation type, and the highest values of G_{23} and G_{13} were found in case of 3D random type orientation. The shear moduli followed the following trend: $G_{12} > G_{13} > G_{23}$.
- The values of elastic as well as shear moduli for hybrid composite were found to be higher than that of Al-9 vol.% RHA. For instance, the value of 2D oriented E_1 increased from 77.15 to 78.40 GPa, and the value of aligned G_{13} enhanced from 29.17 to 29.45 GPa. Therefore, it can be concluded that hybrid composites give luxury to fabricate components with tailored properties at a lower cost.

Declarations

Conflict of interest The authors declare that there are no financial or non-financial interests that are directly or indirectly related to the work submitted for publication.

References

- Fiori G, Iannaccone G, Klimeck G (2006) A three-dimensional simulation study of the performance of carbon nanotube field-effect transistors with doped reservoirs and realistic geometry. *IEEE* 53(8):1782–1788
- Garg P et al (2019) Advance research progresses in aluminum matrix composites: manufacturing & applications. *J Mater Res Technol* 8(5):4924–4939
- Jamwal A et al (2020) Towards sustainable copper matrix composites: manufacturing routes with structural, mechanical, electrical and corrosion behavior. *J Compos Mater* 54(19):2635–2649
- Unterlass MM (2016) Green synthesis of inorganic–organic hybrid materials: state of the art and future perspectives. *Eur J Inorg Chem* 2016(8):1135–1156
- Krishnan PK (2022) Fabrication and application of aluminum metal matrix composites. *Advanced manufacturing techniques for engineering and engineered materials*. IGI Global, Hershey, pp 133–151
- Sharma AK et al. (2020) A study of advancement in application opportunities of aluminum metal matrix composites. In: *Materials today: proceedings*, vol. 26, pp 2419–2424
- Kalra C et al (2018) Processing and characterization of hybrid metal matrix composites. *J Mater Environ Sci* 9.7:1979–1986
- Reddy Panchal M et al (2018) Enhancing compressive, tensile, thermal and damping response of pure Al using BN nanoparticles. *J Alloys Compd* 762:398–408
- Nturanabo F, Leonard M, John BK (2019) Novel applications of aluminum metal matrix composites. *Aluminum alloys and composites*. IntechOpen, London
- Karaoğlu SY, Karaoğlu S, Ünal İ (2021) Aerospace industry and aluminum metal matrix composites. *Int J Aviat Sci Technol* 2.02:73–81
- Prasad SV, Asthana R (2004) Aluminum metal-matrix composites for automotive applications: tribological considerations. *Tribol Int* 17(3):445–453
- Bodunrin MO, Alaneme K, Chown LH (2015) Aluminium matrix hybrid composites: a review of reinforcement philosophies; mechanical, corrosion and tribological characteristics. *J Mater Res Technol* 4(4):434–445
- Budarapu PR, Sudhir Sastry YB, Natarajan R (2016) Design concepts of an aircraft wing: composite and morphing airfoil with auxetic structures. *Front Struct Civil Eng* 10:394–408
- Abdullah E, Bil C, and Watkins S (2009) Application of smart materials for adaptive airfoil shape control. In: 47th AIAA aerospace sciences meeting including the New Horizons forum and aerospace exposition.
- Kumar J et al (2020) Comparative study on the mechanical, tribological, morphological and structural properties of vortex casting processed, Al–SiC–Cr hybrid metal matrix composites for high strength wear-resistant applications: fabrication and characterizations. *J Mater Res Technol* 9.6:13607–13615
- Sarada BN, Srinivasa Murthy PL, and Ugrasen G (2015) Hardness and wear characteristics of hybrid aluminum metal matrix composites produced by stir casting technique. In: *Materials Today: Proceedings*, vol. 2.4–5, pp 2878–2885
- Liu S et al (2019) Effect of B4C and MOS2 reinforcement on the microstructure and wear properties of aluminum hybrid composite for automotive applications. *Compos Part B Eng* 176:107329
- Esawi AMK et al (2010) Effect of carbon nanotube (CNT) content on the mechanical properties of CNT-reinforced aluminum composites. *Compos Sci Technol* 70:2237–2241
- Hashim J, Looney L, Hashmi MSJ (1999) Metal matrix composites: production by the stir casting method. *J Mater Process Technol* 92:1–7
- Sahu MK, Sahu RK (2020) Experimental investigation, modeling, and optimization of wear parameters of B4C and fly-ash reinforced aluminum hybrid composite. *Front Phys* 8:219
- Zhang L et al (2022) On the numerical modeling of composite machining. *Compos Part B Eng* 241:110023
- Sahoo BP, Das D, Chaubey AK (2021) Strengthening mechanisms and modeling of mechanical properties of submicron-TiB2 particulate reinforced Al 7075 metal matrix composites. *Mater Sci Eng A* 825:141873
- Aynalem GF (2020) Processing methods and mechanical properties of aluminum matrix composites. *Adv Mater Sci Eng* 2020:1–19
- Zeng Q, Yu A (2010) Prediction of the mechanical properties of nanocomposites. *Optim Polym Nanocomp Prop*. <https://doi.org/10.1002/9783527629275>
- Tian W et al (2015) Representative volume element for composites reinforced by spatially randomly distributed discontinuous fibers and its applications. *Compos Struct* 131:366–373
- Zhao X et al (2021) Finite element analysis and experiment study on the elastic properties of randomly and controllably distributed carbon fiber-reinforced hydroxyapatite composites. *Ceram Int* 47(9):12613–12622
- Qi L, Tian W, Zhou J (2015) Numerical evaluation of effective elastic properties of composites reinforced by spatially randomly distributed short fibers with certain aspect ratio. *Compos Struct* 131:843–851
- García-Macías E et al (2019) Multiscale modeling of the elastic moduli of CNT-reinforced polymers and fitting of efficiency parameters for the use of the extended rule-of-mixtures. *Compos Part B Eng* 159:114–131
- Kavvadias IE et al (2023) Mechanical characterization of MWCNT-reinforced cement paste: experimental and multiscale computational investigation. *Materials* 16(15):5379
- Frącz W, Janowski G (2019) Predicting effect of fiber orientation on chosen strength properties of wood-polymer composites. *Compos Theory Pract* 19(2):56–63
- Elmarakbi A, Azoti W, Serry M (2017) Multiscale modelling of hybrid glass fibres reinforced graphene platelets polyamide PA6 matrix composites for crashworthiness applications. *Appl Mater Today* 6:1–8

Publisher's Note Springer Nature remains neutral with regard to jurisdictional claims in published maps and institutional affiliations.

Springer Nature or its licensor (e.g. a society or other partner) holds exclusive rights to this article under a publishing agreement with the author(s) or other rightsholder(s); author self-archiving of the accepted manuscript version of this article is solely governed by the terms of such publishing agreement and applicable law.